Composites: Part B 41 (2010) 414–421

Contents lists available at ScienceDirect

Composites: Part B

journal homepage: www.elsevier.com/locate/compositesb

Elastic response of a carbon nanotube fiber reinforced polymeric composite: A numerical and experimental study

Mandar Kulkarni [a], David Carnahan [b], Kapil Kulkarni [b], Dong Qian [c], Jandro L. Abot [a,*]

[a] Department of Aerospace Engineering and Engineering Mechanics, University of Cincinnati, Cincinnati, OH 45221-0070, United States
[b] NanoLab Inc., 55 Chapel Street, Newton, MA 02458, United States
[c] Department of Mechanical Engineering, University of Cincinnati, Cincinnati, OH 45221-0072, United States

ARTICLE INFO

Article history:
Received 20 June 2009
Accepted 28 August 2009
Available online 2 October 2009

Keywords:
A. Nano composite
B. Carbon nanotubes
C. Mechanical properties
C. Numerical analysis

ABSTRACT

Premature failure due to low mechanical properties in the transverse direction to the fiber constitutes a fundamental weakness of fiber reinforced polymeric composites. A solution to this problem is being addressed through the creation of nanoreinforced laminated composites where carbon nanotubes are grown on the surface of fiber filaments to improve the matrix-dominated composite properties. The carbon nanotubes increase the effective diameter of the fiber and provide a larger interface area for the polymeric matrix to wet the fiber. A study was conducted to numerically predict the elastic properties of the nanoreinforced composites. A multiscale modeling approach and the Finite Element Method were used to evaluate the effective mechanical properties of the nanoreinforced laminated composite. The cohesive zone approach was used to model the interface between the nanotubes and the polymer matrix. The elastic properties of the nanoreinforced laminated composites including the elastic moduli, the shear modulus, and the Poisson's ratios were predicted and correlated with iso-strain and iso-stress models. An experimental program was also conducted to determine the elastic moduli of the nanoreinforced laminated composite and correlate them with the numerical values.

1. Introduction

Laminated composite materials consist of a stiff and strong micron-size phase called reinforcement, which is usually a fibrous material like a textile fabric, and another phase called matrix, which is either a polymer, a ceramic, a metal, or a carbon material. A traditional way to improve the properties of polymers and specifically increase their thermal stability and stiffness is to add micron-size fillers. However, a reduction is observed in their ductility, fracture toughness and sometimes strength. In order to avoid those property reductions, nanocomposites can be formed by dispersing nanoparticles in the polymeric matrix: platelets like clay, fibers like carbon nanotube and carbon nanofiber, or particulates like silica or expanded graphite. A considerable improvement in the mechanical properties of the polymer matrix can be achieved with small concentrations of the particles, usually less than 5% by volume. The use of these nanoparticles could however be limited by dispersion problems and viscosity build-up related to strong inter-particle interactions. The particle volume content plays a very important role but the interphase between the matrix and the particles plays an even major role. Among the nanoparticles, the best choice to improve the mechanical properties of the composites is to use carbon nanotubes due to their excellent mechanical, electrical, and thermal properties.

The discovery of fullerenes in the mid 1980s was of great importance in the development of carbon nanotubes [1,2]. Fullerenes are closed cage-like structures of carbon atoms with pentagonal and hexagonal carbon atom rings. The first fullerene was a C_{60} molecule having pentagonal carbon atom rings sharing their sides with adjacent hexagonal carbon atom rings. A few years later, a long fullerene called carbon nanotube (CNT) was first observed by Iijima [3]. Experimental studies reported an average elastic modulus of approximately 1 TPa and an average breaking strength of 30 GPa with an ultimate strain of 5.3% [4]. Other experiments also provided evidence of their high elastic modulus: approximately 1.25 TPa [5], and numerical simulations predicted similar values [6]. It is widely accepted now that CNTs possess exceptionally high mechanical, thermal and electrical properties. CNT-based composites, i.e. CNT nanocomposites, can be fabricated with a wide variety of matrix materials such as polymers, metals and ceramics. In this study, we propose to investigate a CNT nanocomposite as the matrix material of a carbon fiber reinforced polymeric composite to improve its matrix-dominated properties. The resulting nanoreinforced laminated composite is abbreviated as NRLC.

* Corresponding author. Present address: Abot Composites Consulting, 873 Markley Woods Way, Cincinnati, OH 45230, USA. Tel.: +1 (513) 616 3449.
E-mail address: jlabot@gmail.com (J.L. Abot).

1359-8368/$ - see front matter © 2009 Elsevier Ltd. All rights reserved.
doi:10.1016/j.compositesb.2009.09.003

A brief background about CNT nanocomposites, the specific objectives for the study and the multiscale modeling approach to predict the mechanical properties of the NRLC are all presented in the introduction of Section 2. The role of the interfaces in composite materials, the cohesive zone model as a tool to characterize the interface and its formulation are briefly discussed in Section 2.1. Implementation of the cohesive zone model in the Finite Element Method (FEM) and the elasticity-based solution method to evaluate the effective elastic properties of the NRLC are presented in Sections 2.2 and 2.3, respectively. The numerical results are presented in Section 3, and details of the experimental program to mechanically characterize the NRLC and its results are presented in Section 3.5, respectively. Section 4 presents the correlation between the numerical and experimental results. Finally, Section 5 provides a summary and the conclusions of this study.

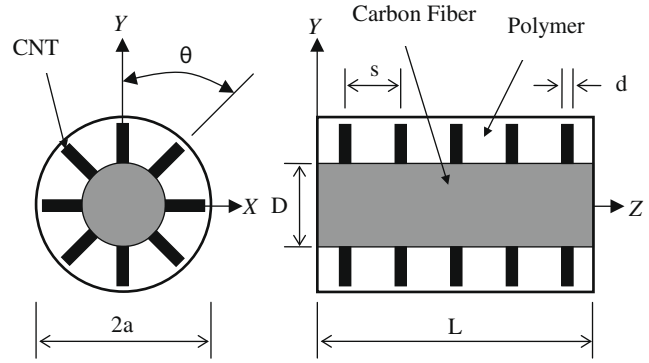

Fig. 2. Schematic illustration of an RVE of NRLC.

2. Materials and numerical formulation

Chemical vapor deposition (CVD) and Nickel catalyst particles are used to grow the carbon nanotubes on the surfaces of carbon fibers [7]. Fig. 1 shows Scanning Electron Microscope (SEM) images of carbon fibers with CNTs grown on their surfaces. These fibers are then impregnated with a polymeric matrix material such as epoxy to fabricate the NRLC samples. Fig. 2 shows a schematic illustration of a representative volume element (RVE) of the NRLC. The carbon nanotubes increase the effective diameter of the fiber and provide a much larger interface area that may improve the fiber/matrix interfacial load transfer characteristics, which in turn should result in higher stiffness and strength of the nanoreinforced polymer matrix surrounding the carbon fiber. Fig. 2 shows also various geometrical parameters that can be chosen during the fabrication process.

The mechanical response of materials is governed by phenomena occurring at different scales of length and time. In nanocomposites, the interactions between the CNTs and the matrix take place at the nanoscale level but they affect the mechanical response of composites at the macroscopic level. Nanoscale phenomena are often studied by molecular dynamics (MD) simulations while behavior at the macroscopic level is conveniently studied with continuum mechanics. MD simulations are limited only to small volumes because of the intensive computational requirements. Therefore, there is a need for multiscale modeling methodologies that relate the molecular and continuum approaches.

In this study, the equivalent macroscopic or continuum-level elastic properties of the NRLC are modeled in two steps. The first step involves modeling the unidirectional nanocomposite consisting of a single CNT surrounded by the polymer matrix and predicting its overall mechanical properties (Fig. 3a). The second step requires modeling the carbon fiber nanoreinforced laminated composite (NRLC) where the matrix is the nanocomposite evaluated in the first step (Fig. 3b). It should be noted that the {*xyz*} coordinate system is used for the nanocomposite description and the {*XYZ*} coordinate system is used for the NRLC description (Fig. 3c).

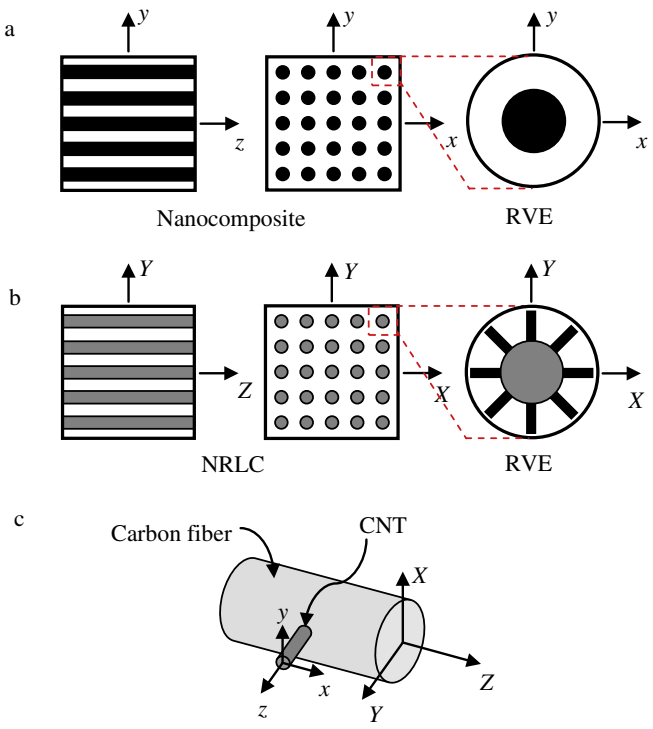

Fig. 3. Schematic illustrations of models to evaluate effective mechanical properties of NRLC: (a) nanocomposite; (b) NRLC; (c) coordinate systems.

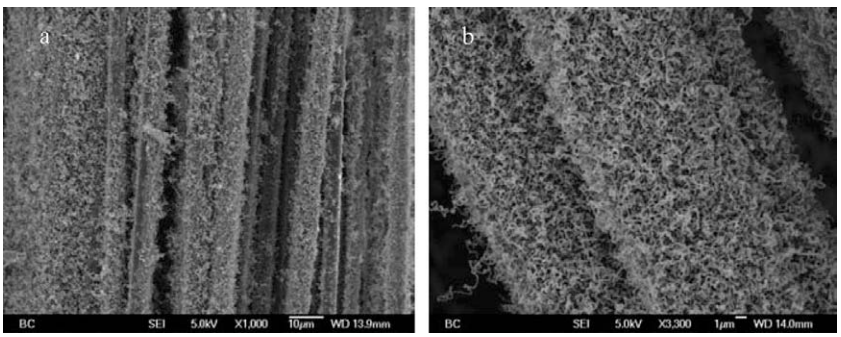

Fig. 1. SEM images of carbon fibers with CNTs grown on their surfaces: (a) fiber bundle; (b) two fibers.

The nanocomposite is a transversely isotropic material with z being the axis of symmetry and the NRLC is transversely isotropic with Z being the axis of symmetry. The nanocomposite properties have to be substituted from the first step into the NRLC model as the matrix properties according to the relation between the two coordinate systems described in Fig. 3c. The interface between CNTs and the polymeric matrix is modeled by the cohesive zone model whose constitutive properties are different than those of the CNTs and the polymer matrix, respectively. The interfacial constitutive properties used here are obtained from MD simulations of CNT pull-out tests ([8–10]). The interface between the carbon fiber and the nanocomposite matrix in the NRLC is also modeled by the cohesive zone approach [11].

An alternative modeling approach could include the use of nanoscale elements that model the material as discrete atoms and chains of atoms with either chemical bond elements based on the Morse Potential or van der Waals elements based on the Lennard–Jones' Potential [12]. This approach would require modeling all three phases of the NRLC and thus be significantly more computationally expensive than the multiscale approach. In another study, Odegard et al. [13] predicted the macroscopic behavior of single-walled carbon nanotube polymeric nanocomposites using an equivalent-continuum modeling approach. First, an equivalent-continuum model of an effective fiber is established based on the numerical results of molecular mechanics to evaluate the material constants. This effective fiber is then used in a continuum model as an inclusion surrounded by polymer to determine the macroscopic properties of the nanocomposite using the Mori–Tanaka method. This model results are compared with those in the present study in Section 3.5. Another approach to evaluate the macroscopic properties of a nanocomposite could be to establish a geometrically equivalent-continuum model of a graphene sheet and determine the thickness of the RVE by equating the energies from MD and continuum methods [14].

2.1. Interface in composites and cohesive zone approach

From a theoretical and computational mechanics point of view, the interface can be broadly classified into two categories: (1) interface with perfect bonding and (2) interface with imperfect bonding. In the case of perfect bonding, the interfacial region is considered to have infinite stiffness and complete load transfer takes place between the fiber and the matrix. The expressions for the average mechanical properties such as elastic moduli, strengths and load sharing between fiber and matrix can be obtained by the rule of mixtures based on the assumptions of iso-strain and iso-stress conditions. These models are built on the average individual stiffnesses of the fiber and the matrix, and their respective volume fractions for a particular composite material. However, these models tend to overestimate the properties since, in reality, the condition of perfect bonding does not prevail and the interface is always of finite stiffness. The interface absorbs part of the externally applied load by undergoing a finite deformation and hence complete load transfer does not take place between the fiber and matrix. It is necessary thus to capture this behavior of the interface to be able to predict the mechanical properties more accurately.

Fracture mechanics principles are traditionally used to characterize the crack propagation at the interface. Linear elastic fracture mechanics (LEFM) [15], J-integral method [16], virtual crack extension (VCE) [17], virtual crack closure (VCC) [18,19] are among the few methods based on fracture mechanics theory. These methods require that the crack be initially present in the model and that the crack propagation path be also specified. Alternatively, techniques can be used to directly introduce fracture mechanisms by adopting softening relationships between tractions and displacements, which in turn introduce a critical fracture energy that is also the energy required to break apart the interfacial surfaces. This technique is called the cohesive zone model and allows solving a fracture mechanics problem such as delamination using continuum mechanics since the displacement field is continuously differentiable across the interface. The interface can be represented by a cohesive zone, i.e., a separate region/surface with zero thickness. A cohesive zone model can be used to characterize its mechanical behavior. The cohesive zone model consists specifically of a constitutive relation between the traction vector, T, acting on the interface and the corresponding interfacial separation, δ, (displacement jump across the interface). It is usual practice to represent the cohesive zone model as a traction–displacement (T—δ) curve.

Barenblatt proposed to describe the fracture process as a material separation across a surface [20]. Similar work was presented by Dugdale in the context of ductile materials such as steel [21]. These works generated a bulk of research activities in an area that is known as cohesive zone model (CZM) in the literature. Many cohesive zone models or cohesive constitutive laws have been developed and referenced [22]. They essentially capture the same phenomenon: as the cohesive surface separates, the traction initially increases reaching a maximum value and then approaches zero as the separation continues to increase. The cohesive zone model was first introduced in FEM by Hillerborg et al. [23].

Depending upon the form of the T—δ functions, CZMs can be categorized as: (i) multilinear; (ii) polynomial; (iii) trigonometric; and (iv) exponential. Volokh used block-peel tests to carry out the comparison between the CZMs based on these functions and reported results that can be found in the literature [22]. It is a common practice to consider the cohesive strength (maximum traction) and the fracture energy or work of separation (area under the traction–displacement curve) as two key parameters in CZMs. The cohesive zone model chosen for this study is the exponential model proposed by Xu and Needleman [24,25]. The cohesive zone model considers the existence of an interfacial potential Φ such that:

$$T = -\frac{\partial \Phi(\Delta)}{\partial \Delta} \tag{1}$$

where $T = T(T_n, T_t)$ = traction vector acting at the cohesive surface; $\Delta = \Delta(\Delta_n, \Delta_t)$ = displacement jump vector.

The potential is of the form:

$$\Phi(\Delta_n, \Delta_t) = \Phi_n + \Phi_n \exp\left(-\frac{\Delta_n}{\delta_n}\right)\left\{\left[1 - r + \frac{\Delta_n}{\delta_n}\right]\frac{1-q}{r-1} - \left[q + \left(\frac{r-q}{r-1}\right)\frac{\Delta_n}{\delta_n}\right] \exp\left(-\frac{\Delta_t^2}{\delta_t^2}\right)\right\} \tag{2}$$

with

$$q = \frac{\Phi_t}{\Phi_n}, r = \frac{\Delta_n^*}{\delta_n} \tag{3}$$

where Φ_n is the work of normal separation and Φ_t is the work of tangential separation. Δ_n^* is the value of Δ_n after complete shear separation under the condition of zero normal tension, $T_n = 0$. The lengths δ_n and δ_t are the characteristic lengths of the cohesive law such that:

$$T_n(\Delta_n) = \sigma_{\max}, \text{ at } \Delta_n = \delta_n \quad \text{when } \Delta_t = 0 \tag{4}$$

$$T_t(\Delta_t) = \tau_{\max}, \text{ at } \Delta_t = \frac{\delta_t}{\sqrt{2}} \quad \text{when } \Delta_n = 0 \tag{5}$$

$\sigma_{\max}$ and $\tau_{\max}$ are the interface normal and tangential strengths, respectively. Expressions of the normal and tangential tractions at the interface can be obtained by combining Eqs. (2) and (3) and are given by:

$$T_n = \frac{\Phi_n}{\delta_n}\exp\left(-\frac{\Delta_n}{\delta_n}\right)\left\{\frac{\Delta_n}{\delta_n}\exp\left(-\frac{\Delta_t^2}{\delta_t^2}\right)+\frac{1-q}{r-1}\left[1-\exp\left(-\frac{\Delta_t^2}{\delta_t^2}\right)\right]\left[r-\frac{\Delta_n}{\delta_n}\right]\right\} \quad (6)$$

$$T_t = 2\left(\frac{\Phi_n\Delta_t}{\delta_t^2}\right)\left\{q+\left(\frac{r-q}{r-1}\right)\frac{\Delta_n}{\delta_n}\right\}\exp\left(-\frac{\Delta_n}{\delta_n}\right)\exp\left(-\frac{\Delta_t^2}{\delta_t^2}\right) \quad (7)$$

The areas under the normal traction–separation curve and the shear traction–separation curve represent the work of normal separation, Φ_n, and shear separation, Φ_t, respectively. The latter is the energy required for complete separation. From Eqs. (5) and (6), it can be shown that Φ_n and Φ_t take the form:

$$\Phi_n = \exp(1)\sigma_{\max}\delta_n, \Phi_t = \sqrt{\frac{\exp(1)}{2}}\tau_{\max}\delta_t \quad (8)$$

The values of the parameters q and r are usually selected to reduce the computational efforts.

2.2. RVE for finite element modeling

The mechanical behavior of composites can be effectively studied using an RVE that consists of a single carbon fiber or CNT surrounded by matrix material. Mainly, three types of RVEs can be found in the literature [26]: (a) cylindrical; (b) square; and (c) hexagonal. Square and hexagonal RVEs are believed to yield the best results because of their ability to fill the space as compared to the cylindrical RVE. It is also shown in the literature that cylindrical RVEs tend to overestimate the elastic modulus of the composites compared to the numerical results obtained from a square RVE [26,27]. However, several studies have been carried out using cylindrical RVEs due to the availability of analytical solutions and 2D axisymmetric FEM models that can reduce computational time. In this study, a hierarchical approach employing a cylindrical RVE is considered to exploit the axisymmetric nature of the NRLC. However, some loading cases will require a full scale 3D cylindrical RVE due to the incorporation of cohesive zone elements in the FEM model and due to limitations of the FEM code (ANSYS™). Fig. 4 shows the cut-through section of the cylindrical RVE with the corresponding coordinate system.

2.3. The elasticity model for evaluation of elastic properties

CNTs and the polymer matrix are considered as homogeneous and isotropic materials while the carbon fibers are considered as transversely isotropic materials with known elastic moduli and Poisson's ratios. All the materials are assumed to behave linearly elastically. It is assumed that the CNTs and the carbon fibers are imperfectly bonded to the matrix material in the respective models: the bonds between CNTs and the polymer matrix and between carbon fibers and the polymer matrix are of finite stiffness. With these assumptions, the homogenized solid composite material becomes transversely isotropic in both models (see compliance tensor in Eq. (9)). Fig. 4 shows the coordinate system orientation where z is the axis of symmetry.

$$\begin{bmatrix} \frac{1}{E_x} & -\frac{\upsilon_{xy}}{E_x} & -\frac{\upsilon_{xz}}{E_x} & 0 & 0 & 0 \\ -\frac{\upsilon_{yx}}{E_y} & \frac{1}{E_y} & -\frac{\upsilon_{yz}}{E_y} & 0 & 0 & 0 \\ -\frac{\upsilon_{zx}}{E_z} & -\frac{\upsilon_{zy}}{E_z} & -\frac{1}{E_z} & 0 & 0 & 0 \\ 0 & 0 & 0 & \frac{1}{G_{xz}} & 0 & 0 \\ 0 & 0 & 0 & 0 & \frac{1}{G_{yz}} & 0 \\ 0 & 0 & 0 & 0 & 0 & \frac{2(1+\upsilon_{xy})}{E_x} \end{bmatrix} \quad (9)$$

where

$$\frac{\upsilon_{zx}}{E_z} = \frac{\upsilon_{xz}}{E_x} = \frac{\upsilon_{zy}}{E_z} = \frac{\upsilon_{yz}}{E_y} \quad \text{and} \quad E_x = E_y, \upsilon_{xz} = \upsilon_{yz}, G_{xz} = G_{yz} \quad (10)$$

Five independent elastic properties, namely, two elastic moduli, E_x and E_z, two Poisson's ratios, υ_{xy}, and υ_{zx}, and a shear modulus, G_{xz}, are required to completely characterize the mechanical response of the transversely isotropic material. Five equations are thus needed to determine these five properties. Four equations are developed to evaluate the two elastic moduli, E_x and E_z, and the two Poisson's ratios, υ_{xy} and υ_{zx}, by considering three loading cases for the cylindrical RVE. The RVE corresponding to a multiwalled carbon nanotube in the nanocomposite is assumed to be a solid cylinder with length L, radius R, and CNT radius r. Multiwalled CNTs are assumed to be solid to simplify the model and the calculations. Liu et al. used this approach for a hollow cylindrical RVE and developed a set of equations to determine the elastic properties [26]. The present study is an extension of this approach for solid cylindrical RVEs. A fifth equation is developed to evaluate the shear modulus, G_{yz}, by using the plane stress condition.

2.3.1. Plane stress loading case for evaluation of G_{yz}

Consider a thin plate from the RVE shown as the shaded area in Fig. 5. In this loading case, the plate is fixed at the bottom surface (in x–z plane) and subjected to a shear stress σ_{yz} at the top. This gives rise to a plane stress condition with $\sigma_{xx} = \sigma_{yy} = 0$. From Eq. (9):

$$G_{yz} = \frac{\sigma_{yz}}{\gamma_{yz}} \quad (11)$$

where γ_{yz} is the average shear strain, which is given by:

$$\gamma_{yz} = \frac{1}{R}\int_0^R \frac{u_z(y)}{y}dy \quad (12)$$

Eq. (12) is valid for small deformations and can be obtained from FEM results.

3. Numerical results

A cylindrical RVE consisting of a single CNT/carbon fiber surrounded by polymer/nanocomposite matrix is studied with the FEM to determine the effective elastic properties of the nanocomposite/NRLC. The commercial code ANSYS™ is used to create and

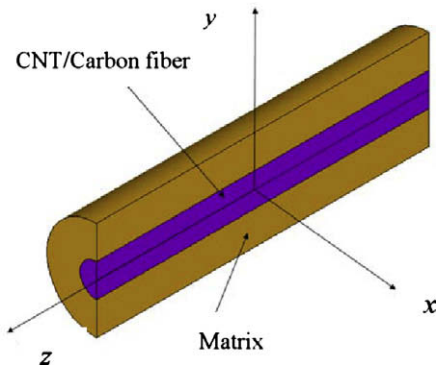

Fig. 4. Schematic illustration of cylindrical RVE with corresponding coordinate system.

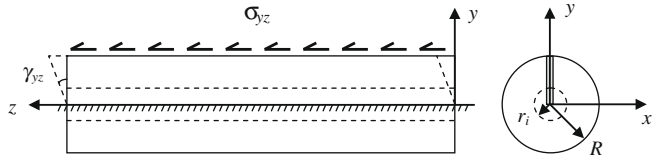

Fig. 5. Schematic illustration of thin plate under shear stress σ_{yz}.

analyze the FEM model of the RVE. Different boundary conditions are applied to the RVE as described in the previous section, and then the FEM results are post-processed to obtain the elastic properties.

3.1. Finite element modeling with cohesive zone elements

Two-dimensional axisymmetric models are considered for axial and lateral loading [23] due to the axisymmetric nature of the RVE geometry and loading. Although the axisymmetric model significantly reduces the computational time, a full scale 3D FE model is needed for the case of torsional loading [26]. The latter is a case of axisymmetric geometry with antisymmetric loading. The elements to be used to model this condition need to exhibit axisymmetric nature with a minimum of three translational degrees of freedom (DOFs) at each node, in the x, y and z directions, respectively. Two-dimensional cohesive zone elements currently available in the ANSYS™ element library are not capable of representing this loading condition due to the lack of translational DOF in the z-direction. Finally, a 2D plane stress model is considered for the shear loading case (Fig. 5). In the case of axisymmetric and plane stress models, 2D 8-node Quad elements are used to model the CNT/carbon fiber and the matrix with a single layer of 2D 6-node cohesive zone elements in between them to model the interface. Fig. 6a and b show the finite element meshes used in the models. 3D 20-node Brick elements are used to model the CNT/carbon fiber and the matrix with a single layer of 3D 16-node cohesive zone elements in between them to simulate the interface in the case of torsional loading (Fig. 6c).

3.2. Cohesive zone elements in ANSYS^{R}

The discussion in this section is restricted to the cohesive zone elements used in this study: 2D 6-node quadratic interface element and 3D 16-node quadratic interface element, respectively. There are many other cohesive zone elements available in the ANSYS™ element library and their use depends upon the nature of the problem at hand. A cohesive zone element or the interface element in ANSYS™ consists of top and bottom surfaces. The top and bottom surfaces coincide initially, i.e., nodes on the top and bottom surfaces coincide with each other at the respective locations. They also coincide with the nodes of the adjacent structural elements. The fracture or delamination is represented by the separation between the top and bottom surfaces and characterized by the increasing displacement between the nodes of the top and bottom surfaces within the interface element itself. This phenomenon is governed by the previously described exponential constitutive law or the cohesive zone model. By choosing appropriate values for q and r, the simplified form of Eq. (3) is given by:

$$\Phi(\Delta) = e\sigma_{\max}\delta_n\left[1-\left(1+\frac{\Delta_n}{\delta_n}\right)e^{-\left(\frac{\Delta_n}{\delta_n}\right)}e^{-\left(\frac{\Delta_t}{\delta_t}\right)^2}\right] \tag{13}$$

Δ_n and Δ_t, are the variables in this relation and the only parameters that determine the form of the $T-\delta$ curve are $\sigma_{\max}, \delta_n$ and δ_t. These parameters are input into the ANSYS^{R} model to define the constitutive behavior of the above mentioned cohesive zone elements. It should be noted that the values of these parameters can be extracted from the $T-\delta$ plots available from MD simulations as explained earlier.

3.3. Numerical results for CNT–polymer nanocomposite

First, the response of the nanocomposite is studied using the RVE. A multiwalled CNT is considered for the analysis and is modeled as a solid cylinder having a radius of $r_i = 5$ nm and a length of $L = 100$ nm. For the matrix, the dimensions are: $R = 15$ nm and $L = 100$ nm. These dimensions are chosen based upon the values used in previous studies to evaluate the behavior of the composite RVE [26]. Both the CNT and the matrix are assumed to be homogeneous, isotropic and linearly elastic materials with the elastic modulus and Poisson's ratio being: $E_{CNT} = 1$ TPa, $\nu_{CNT} = 0.3$, $E_{matrix} = 3$ GPa and $\nu_{matrix} = 0.3$. These values are the representative ones for carbon nanotubes [4,5,7,8,10,26] and for an epoxy polymer like the one used in the experimental section of this study. Two CNT volume fractions were considered: 2% and 11%, respectively. The latter is comparatively higher than those typically used in nanocomposites but it is important to keep in mind that buckypaper and other composite systems could reach volume fractions up to 40%. The constitutive behavior of the cohesive zone elements is defined by using the following input parameters: $\sigma_{max} = 1$ GPa, $\delta_n = 1.2$ nm, $\delta_t = 1.2$ nm. σ_{max} is the peak normal traction attained at the interface elements where the initiation of damage takes place. δ_n is the normal separation between the nodes of the interface element where the peak normal traction occurs, and δ_t is the tangential separation between the nodes of the interface element such that the peak tangential traction occurs at $\delta_t/\sqrt{2}$. These values are the representative values of the interface strength where carbon nanotubes are chemically bonded to the matrix material. Chandra et al. showed that the interface strength value ranges from 500 MPa to 5 GPa depending upon the density of the chemical bonds per unit length of the CNT [9]. The FEM results for the effective elastic properties of the transversely isotropic nanocomposite are summarized in Table 1.

These results are in good agreement with the values reported in the literature [9] and confirm that significant reductions in the effective mechanical properties of nanocomposites are observed when the bonding between the CNTs and the polymer matrix is

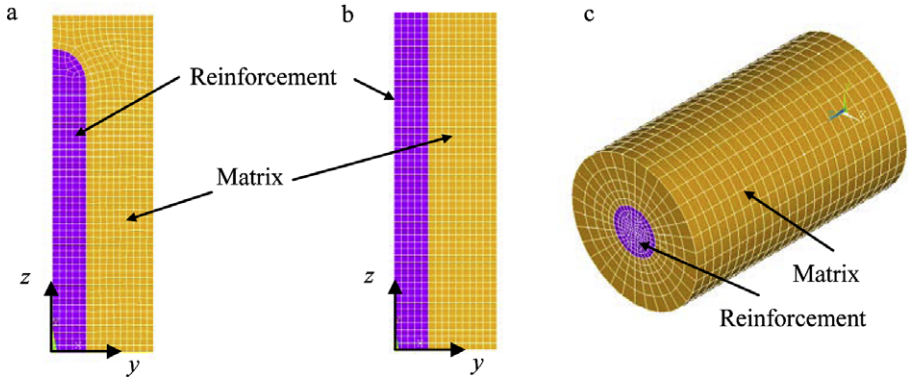

Fig. 6. FE meshes for: (a) axial loading; (b) lateral and shear loading; (c) torsional loading.

considered to be imperfect, which is the actual case [10,26]. Liu et al. [26] had predicted the nanocomposite properties in the case of perfect bonding for different values of matrix elastic moduli with $E_{CNT} = 1$ TPa. Their studies considered: $E_{matrix} = 5$ GPa with about 5% CNT volume fraction, yielding $E_z = 53.5$ GPa, which was approximately 10 times the elastic modulus of the matrix. Also, E_x was predicted to be 3.75 times the value of E_{matrix}. The work by Liu et al. employed the cohesive zone model implemented within the framework of the Boundary Element Method (BEM) to predict the nanocomposite elastic properties [10]. With carbon nanotubes considered as rigid inclusions in the matrix, a 50% reduction is reported in the elastic properties for a weaker interface compared to the strong or perfectly bonded interface for a specific CNT volume fraction. The FEM results of our study with the cohesive zone model show a significant reduction in the elastic moduli comparable to those described in the literature [26]. The cohesive zone model, thus, is capable of capturing the effect of imperfect bonding in numerical simulations and can be considered as an efficient tool to represent the interface in composite materials. Further consideration of the numerical results entails understanding that the effective elastic properties of the nanocomposite are sensitive not only to the cohesive zone model but also to the MD simulations used to build it.

3.4. Effect of interfacial strength and volume fraction on elastic moduli

The interface strength plays a major role in determining the elastic properties of the nanocomposite. A numerical study was carried out to learn the effect of the interface strength on the longitudinal elastic modulus of the nanocomposite for different values of CNT volume fractions. Fig. 7 shows the curves of E_z versus the CNT volume fraction for different values of the interface strength. Theoretical bounds exist for the interface strength in composite materials. The lower bound for the interface strength is zero, which corresponds to the case where there is no load transfer from the polymeric matrix to the CNT and the equivalent properties of the composite become those of the matrix material. The upper bound for the interface strength is infinity, which represents the case of perfect bonding where there is complete load transfer from the polymeric matrix yielding ideal composite material properties. Only finite values of the interface strength are presented in Fig. 7.

It is observed from these curves that by keeping the interface strength constant, the elastic modulus of the nanocomposite increases with increasing volume fraction of the CNTs as expected. Initially, the elastic modulus increases at a faster rate and becomes almost constant after a certain volume fraction. Also, for a particular value of the CNT volume fraction, the modulus of the nanocomposite increases with increasing interface strength. Again, the rate of increase in the modulus of the nanocomposite reduces with increasing interface strength. It should be noted that the different values used of the interface strength in the present study do not correspond to any of the actual values obtained from the MD simulations.

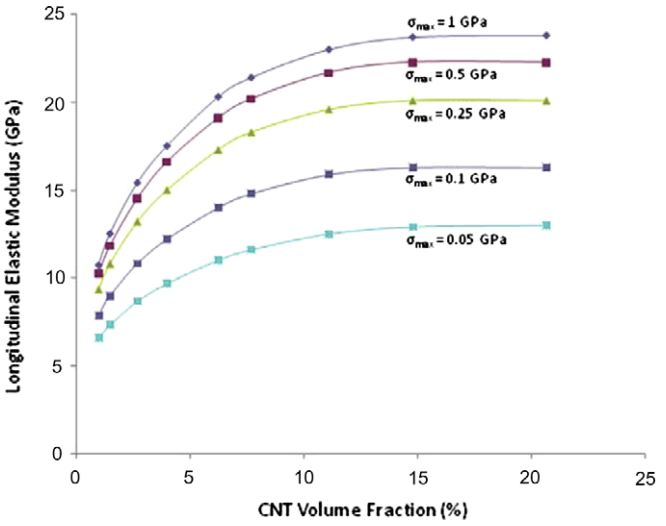

Fig. 7. Effect of interface strength and CNT volume fraction on the longitudinal elastic modulus of the nanocomposite.

3.5. Numerical results for nanoreinforced laminated composite

Once the nanocomposite is completely characterized, it is considered as the matrix material for modeling of the NRLC and calculating its effective mechanical properties. IM7 is the selected carbon fiber, which is a transversely isotropic material with the elastic properties given in Table 2. The resulting NRLC with IM7 carbon fiber as the reinforcement phase and the nanocomposite as the matrix phase is also a transversely isotropic material. Hence, the same approach that was used to predict the elastic properties of the nanocomposite will be considered to predict those of the NRLC including the same four loading conditions, the theory of elasticity, and the FEM.

The cohesive zone approach is also used to represent the interface between the carbon fiber and the nanocomposite matrix. The determination of input parameters for the cohesive zone model is particularly critical but no definite values are currently available. In our study, the value of σ_{max} is assumed to be equal to one tenth of the elastic modulus of the carbon fiber in the transverse direction, E_X. Xu and Needleman assumed the normal cohesive interface strength as 10% of the elastic modulus of PMMA (poly-methylmethacrylate) in their numerical simulations of fast crack growth in brittle solids [25]. In a study of impact-induced delamination of composites, a somewhat smaller value for the cohesive interface strength was used: 0.5% of the transverse elastic modulus of the fiber reinforced polymeric composite material itself [11]. The constitutive behavior of the cohesive zone elements for this study is defined by using the following input parameters: $\sigma_{max} = 1.85$ GPa (10% of E_X of IM7), $\delta_n = l.2$ nm, $\delta_t = 1.2$ nm. The FEM results for the effective elastic properties of the NRLC are summarized in Table 3.

Table 1
Elastic properties of CNT nanocomposite predicted by FEM.

Property	Value (11% CNT)	Value (2% CNT)
E_z	23.00 GPa	13.70 GPa
ν_{zx}	0.28	0.29
E_x	7.22 GPa	4.71 GPa
V_y	0.14	0.14
G_{yz}	4.20 GPa	1.49 GPa

Table 2
Elastic properties of IM7 carbon fiber for modeling effort.

Property	Value
E_Z	294.00 GPa
ν_{ZX}	0.27*
E_X	18.50* GPa
ν_{XY}	0.30
G_{yz}	25.00* GPa

* Estimated property.

These results show that it is possible to improve the matrix-dominated properties of fiber reinforced polymeric composites with the use of a nanocomposite matrix material. With 11% IM7 fiber and 11% CNT volume fractions, respectively, the elastic modulus of the NRLC in the transverse direction, E_X increases to almost six times the value of the polymer matrix. A more common composite with 41% IM7 fiber and 2% CNT volume fractions, respectively, yields a transverse modulus of about four and a half times that of the polymer matrix. The elastic modulus of composites in the transverse direction to the fiber is usually well predicted by the iso-stress model and the results of this study are within 30% error. The longitudinal elastic modulus, E_Z, of composites is well predicted with the iso-strain model, which assumes perfect bonding between the fibers and the matrix. It will give a value of 38.77 GPa for 11% volume fraction of IM7 carbon fiber. The predicted elastic modulus for the NRLC from FEM is 42.80 GPa. This corresponds to a 10% increase in the longitudinal elastic modulus that can be obtained with this CNT nanocomposite. In the case of 41% IM7 fiber content however, the predicted longitudinal elastic modulus of the NRLC is 33% lower than that determined with the iso-strain model. This modulus would also be lower than the one predicted by Odegard [13] due to different assumed potentials in the MD simulation and also different homogenization techniques. The value of the out-of-plane Poisson's ratio, υ_{ZX}, is 0.16 for both volume fractions. It is lower than the Poisson's ratios of any of the phase materials. Both the elastic modulus in the fiber direction and the out-of-plane Poisson's ratio are usually well predicted by the iso-strain model but are underestimated in this study. The value for the Poisson's ratio in the plane of isotropy, υ_{XY}, of 0.34 for 41% IM7 fiber content is in line with that of a composite material, but the value of 0.47 for 11% IM7 fiber content is too high. The latter is attributed to the high value of $\sigma_{\max}$ in the cohesive zone model. Further studies with different values of the model parameters are needed to determine their effect on the elastic properties of the composite. In addition, the effect of increasing CNT volume fractions on the longitudinal elastic modulus needs to be studied in more detail and correlated with previous studies [13].

Multiwalled CNTs are assumed to be solid to simplify the problem but in reality, they consist of graphene sheets rolled into seamless cylinders arranged concentrically one inside the other, with typically hemispherical end caps. Adjacent walls of the CNT are attached to each other by van der Waals forces. Only the outermost graphene sheet is attached to the polymeric matrix. Therefore, the assumption of solid CNTs is not completely valid and introduces an additional stiffness into the NRLC. Also, the CNTs are assumed to be homogeneous, linearly elastic and isotropic. They represent only an approximation to their mechanical behavior but are widely accepted due to the limited availability of experimental data.

4. Experimental program and results

Experiments were performed to determine the mechanical properties of a unidirectional NRLC and in particular the elastic modulus in the transverse direction to the fiber, E_X. IM7 carbon fibers were used to grow carbon nanotubes on them and Epon862 was used as the polymer matrix with LS81K hardener. Several functionalization schemes were considered to achieve the best possible bonding of the nanotubes. The prepared composite plates had a fiber volume fraction of approximately 40% and a CNT volume fraction of approximately 2%. NRLC plates were fabricated using a resin transfer molding process and samples were cut from the plates having uniform rectangular cross-section for tensile testing. The strain was measured by means of strain gages and the load value was recorded and monitored by a load cell. Stress values were then calculated from the recorded load values based upon the sample's cross-sectional dimensions. Fig. 8 shows a representative stress–strain curve of a unidirectional NRLC subjected to uniaxial loading in the transverse direction to the fiber. The slope of this curve corresponds to the effective elastic modulus of the composite. Table 4 presents the statistically analyzed experimental results including the elastic modulus, strength and ultimate strain.

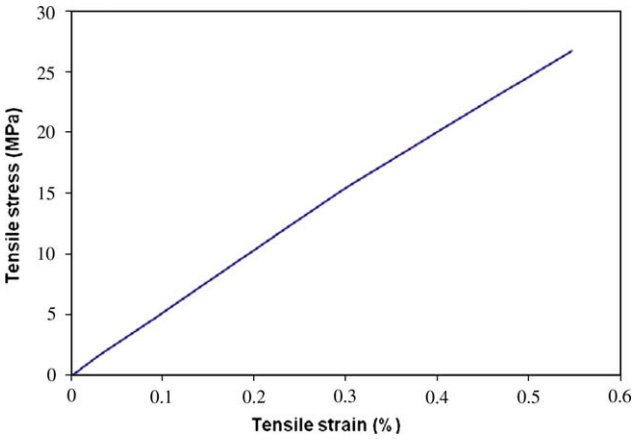

Fig. 8. Stress–strain curve of aminopyrene functionalized CNT/IM7/Epon862(LS81K) unidirectional NRLC subjected to uniaxial quasi-static loading in the transverse direction to the fiber (sample dimensions: length of 75 mm with gage length of 50 mm; width of 7.5 mm; and thickness of 2.5 mm).

5. Correlation of numerical and experimental results

The elastic properties of the NRLC were predicted and experimentally determined using 2% CNT volume fraction and about 40% fiber volume fraction. From the experimental results, it was determined that the highest value of the elastic modulus in the transverse direction to the fiber was for an aminopyrene functionalized CNT/carbon fiber/epoxy NRLC with a mean value of 10.02 GPa. The numerical analysis predicted the elastic modulus in the transverse direction to be about 1.4 times the experimentally determined value. This error could be attributed to the assumptions of the multiscale model but also to improper bonding of the nanotubes to the fiber during the manufacturing of the NRLC plate.

The interface strength considered in the numerical study was drawn from MD simulations of CNT pullout tests. MD simulations provide enough details about the interface. However, the results still need to be validated with the experimental results. More

Table 3
FEM results for NRLC.

Property	Value (11% CNT; 11% IM7 fiber)	Value (2% CNT; 41% IM7 fiber)
E_Z	42.80 GPa	83.60 GPa
υ_{ZX}	0.16	0.16
E_X	17.49 GPa	13.93 GPa
υ_{XY}	0.47	0.34
G_{YZ}	7.88 GPa	9.36 GPa

Table 4
Experimentally-determined mechanical properties of aminopyrene functionalized CNT/TM7/Epon862(LS81K) unidirectional NRLC.

	$E_2 = E_x$ (GPa)	$\sigma_{22ult} = \sigma_{XXult}$ (MPa)	$\epsilon_{22ult} = \epsilon_{XXult}$ (%)
Average	10.02	29.07	0.28
Std. Dev.	1.13	3.23	0.05

advanced MD simulations are needed to study the CNT–polymer interface in detail and to be able to define the cohesive zone model. Also, the cylindrical RVE used for numerical studies tends to overestimate the overall composite material properties as compared to the hexagonal and square RVEs because of the left out material in the corners. More elaborate techniques for the manufacturing of the nanoreinforced laminated composites are also required to yield good quality composite plates for the experimental characterization work. A better polymer wetting of the carbon nanotubes and the carbon fibers will also ensure greater load transfer between all phases.

6. Conclusions

A novel CNT nanoreinforced laminated composite, NRLC, was designed to improve the matrix-dominated properties of fiber reinforced polymeric composites. Its mechanical response was investigated and the most relevant results were presented in this study. It included a combined numerical approach using a multiscale modeling method and an experimental program. It was determined that multiscale modeling can be effectively and conveniently used to study nanoreinforced laminated composites. Incorporation of the cohesive zone model in the finite element model captures the interfacial behavior adequately and provides more accurate results than perfect bonding models. The CNT–polymer interfacial strength and the volume fractions of the CNT and microfiber reinforcements play the most important role in the mechanical response of the NRLC. The elastic modulus of a fiber reinforced composite in the transverse direction to the fiber can usually be improved about three times respect to the value of the pure polymer matrix. FEM results for the NRLC show that there is a possibility of improving the matrix-dominated properties of conventional fiber reinforced composites with the use of a nanocomposite matrix material. It was shown that the elastic modulus of the NRLC in the transverse direction to the fiber increases several fold respect to the value of the polymer matrix with the addition of about 10% CNT volume content. The results of this study also indicate that the elastic modulus in the transverse direction to the fiber can be better predicted than the elastic modulus in the fiber direction and the Poisson's ratios.

Acknowledgements

The experimental section of this study was conducted with the financial support of Grant N00014-08-M-0324 from the Office of Naval Research. The support of program manager, Dr. Ignacio Perez, is greatly appreciated.

References

[1] Kroto HW, Heath JR, O'Brien SC, Curl RF, Smalley RE. C60: Buckminsterfullerene. Nature 1985;318:162–3.
[2] Thostenson ET, Chou T-W. Aligned multi-walled carbon nanotube-reinforced composites: processing and mechanical characterization. J Phys D Appl Phys 2002;35(16):77–80.
[3] Iijima S. Helical microtubules of graphitic carbon. Nature 1991;354:56–8.
[4] Yu M-F, Files BS, Arepalli S, Ruoff RS. Tensile loading of ropes of single wall carbon nanotubes and their mechanical properties. Phys Rev Lett 2000;84(24):5552–5.
[5] Krishnan A, Dujardin E, Ebbesen TW, Yianilos PN, Treacy MMJ. Young's modulus of single walled nanotubes. Phys Rev B 1998;58(20):14013–9.
[6] Robertson DH, Brenner DW, Mintmire JW. Energetics of nanoscale graphitic tubules. Phys Rev B 1992;45(21):12592–5.
[7] Thostenson ET, Li WZ, Wang DZ, Ren ZF, Chou TW. Carbon nanotube/carbon fiber hybrid multiscale composites. J Appl Phys 2002;91(9):6034–7.
[8] Chandra N, Namilae S. Multiscale model to study the effect of interfaces in carbon nanotube based composites. J Eng Mater – T ASME 2005;127(2):222–32.
[9] Chandra N. Cohesive zone approach to multiscale modeling of nanotube reinforced composites. Florida A&M University, Project No. 37-1906-041 (FAMU 37099); 2004.
[10] Liu YJ, Nishimura N, Qian D, Adachi N, Otani Y, Mokashi V. A boundary element method for the analysis of CNT/polymer composites with a cohesive interface model based on molecular dynamics. Eng Anal Bound Elem 2007;32(4):299–308.
[11] Geubelle PH, Baylor JS. Impact induced delamination of composites: a 2D simulation. Compos Part B – Eng 1998;29B(5):589–602.
[12] Wang Y, Sun C, Sun X, Hinkley J, Odegard GM, Gates TS. 2-D nano-scale finite element analysis of polymer field. Compos Mater Sci 2003;63(ll):1581–90.
[13] Odegard GM, Pipes RB, Hupert P. Comparison of two models of SWCN polymer composites. Compos Mater Sci 2004;64(7-8):1011–20.
[14] Odegard GM, Gates TS, Nicholson LN, Wise KE. Equivalent continuum modeling of nano-structured materials. Compos Mater Sci 2002;62(14):1869–80.
[15] Anderson TL. Fracture mechanics: fundamentals and applications. Boca Raton, FL: Taylor & Francis; 2005.
[16] Rice JR. A path independent integral and the approximate analysis of strain concentration by notches and cracks. J Appl Mech – T ASME 1968;35:379–86.
[17] Hellen TK. On the method of virtual crack extension. Int J Numer Methods Eng 1975;9(1):187–207.
[18] Rybicki EF, Kanninen MF. A finite element calculation of stress intensity factors by a modified crack closure integral. Eng Fract Mech 1977;9:931–8.
[19] Raju IS. Calculation of strain-energy release rates with higher order and singular finite elements. Eng Fract Mech 1987;28(3):251–74.
[20] Barenblatt GI. The mathematical theory of equilibrium cracks formed in brittle fracture. Adv Appl Mech 1962;7(42):55–129.
[21] Dugdale DS. Yielding of steel sheets containing slits. J Mech Phys Solids 1960;8(2):100–4.
[22] Volokh KY. Comparison between cohesive zone models. Commun Numer Methods Eng 2004;20(ll):845–56.
[23] Hillerborg A, Moder M, Petersson PE. Analysis of crack formation and crack growth in concrete by means of fracture mechanics and finite elements. Cement Concrete Res 1976;6(6):773–82.
[24] Xu XP, Needleman A. Void nucleation by inclusion debonding in a crystal matrix. Model Simul Mater Sci 1993;1(2):111–32.
[25] Xu X-P, Needleman A. Numerical simulations of fast crack growth in brittle solids. J Mech Phys Solids 1994;42(9):1397–434.
[26] Liu YJ, Chen XL. Evaluations of the effective material properties of carbon nanotube-based composites using a nanoscale representative element. Mech Mater 2003;35(l-2):69–81.
[27] Chen XL, Liu YJ. Square representative volume elements for evaluating the effective material properties of carbon nanotube-based composites. Compos Mater Sci 2004;29(l):1–11.